Society for Mathematical Biology

CrossMark

Neutral Genetic Patterns for Expanding Populations with Nonoverlapping Generations

Nathan G. Marculis[1] · **Roger Lui**[2] ·
Mark A. Lewis[1,3]

Abstract We investigate the inside dynamics of solutions to integrodifference equations to understand the genetic consequences of a population with nonoverlapping generations undergoing range expansion. To obtain the inside dynamics, we decompose the solution into neutral genetic components. The inside dynamics are given by the spatiotemporal evolution of the neutral genetic components. We consider thin-tailed dispersal kernels and a variety of per capita growth rate functions to classify the traveling wave solutions as either pushed or pulled fronts. We find that pulled fronts are synonymous with the founder effect in population genetics. Adding over-compensation to the dynamics of these fronts has no impact on genetic diversity in the expanding population. However, growth functions with a strong Allee effect cause the traveling wave solution to be a pushed front preserving the genetic variation in the population. In this case, the contribution of each neutral fraction can be computed by a simple formula dependent on the initial distribution of the neutral fractions, the traveling wave solution, and the asymptotic spreading speed.

Keywords Integrodifference equations · Neutral genetic diversity · Range expansion · Traveling wave · Founder effect · Allee effect

✉ Nathan G. Marculis
    marculis@ualberta.ca

[1] Department of Mathematical and Statistical Sciences, Centre for Mathematical Biology, University of Alberta, Edmonton, AB T6G 2G1, Canada

[2] Department of Mathematical Sciences, Worcester Polytechnic Institute, Worcester, MA 01609, USA

[3] Department of Biological Sciences, University of Alberta, Edmonton, AB T6G 2G1, Canada

1 Introduction

The topic of populations undergoing range expansions in spatial ecology is well studied (Holmes et al. 1994; Ibrahim et al. 1996; Thomas et al. 2001). However, many of the previous mathematical studies focus on the spread of entire populations and ignore the neutral genetic consequences of the expansion (Kot 1992; Lutscher 2008; Wang et al. 2002). The aim of this work is to connect the range expansion of a population to the genetic consequences for populations with nonoverlapping generations. To achieve this goal, we develop and analyze a mathematical model of integrodifference equations to connect the fundamental ecological and genetic concepts with mathematical structure.

A recent interest in ecological literature is focused around the neutral genetic consequences of range expansions (Hallatschek and Nelson 2008). A founder effect is said to occur when the establishment of a new population is performed by a few original founders who carry only a small fraction of the total genetic variation of the parental population (Mayr 1942). It is a widely accepted notion that range expansions often lead to a loss of genetic diversity because of the founder effect (Dlugosch and Parker 2008; Ibrahim et al. 1996). Serial founder events that occur when a population undergoes a range expansion result in the phenomena known as gene surfing (Excoffier and Ray 2008). This is the spatial analog of genetic drift and occurs when alleles reach higher than expected frequencies at the front of a range expansion (Slatkin and Excoffier 2012). By understanding the effect that spatial assortment plays in expanding populations, we can begin to understand the effect that dispersal has on genetic diversity, independent of selection.

It has been shown that, in some scenarios, genetic drift in edge populations can be a stronger driver than selection during range expansion because of the spatial structure of the population (Müller et al. 2014). A simple theoretical experiment was conducted to demonstrate that mutations at expanding frontiers can sweep through a population, even without any selective advantage (Hallatschek et al. 2007). This experiment provides support for theoretical arguments and genetic evidence that common genes in a population may not necessarily reflect positive selection but, instead, may be due to recent range expansions (Hewitt 2000). This evidence motivates the work conducted in this paper to understand the effect that growth and dispersal have on the neutral genetic composition of a population.

Often, large scale genomic surveys are motivated, in part, by the idea that the neutral genetic variation observed in a population may be used to reconstruct the history of its range expansion (Hewitt 1996). However, the ability to trace back the colonization pathways of a species from their genetic footprints is limited by our understanding of the genetic consequences of a range expansion (Excoffier 2004; Hallatschek and Nelson 2008). The model considered in this work provides a framework for understanding the genetic consequences that in turn can assist the inverse problem of understanding where the species originated.

Mathematically, the concept of modeling the evolution of the neutral genetic diversity of an expanding population is known as the "inside dynamics" of the population. The term comes from the idea that we break the population into subpopulations that can be identified by a neutral genetic marker used to study the underlying structure of the population. A recent series of papers focused on understanding the inside dynamics

for a variety of different types of continuous-time models (Garnier et al. 2012; Roques et al. 2012; Bonnefon et al. 2013, 2014). Early work on inside dynamics focused on the study of the classical reaction diffusion equations with monostable, bistable, or ignition type reaction dynamics. The authors were able to classify the inside dynamics of the deterministic population structure in terms of pulled and pushed traveling wave solutions (Garnier et al. 2012). The theory was quickly extended by incorporating biological insight to the original work by showing that Allee effects preserve genetic diversity (Roques et al. 2012). The inside dynamics analysis has also been extended to other kinds of scalar equations such as delayed traveling waves (Bonnefon et al. 2013) and integrodifferential equations (Bonnefon et al. 2014).

As was done for the previous studies on continuous-time models, this work aims to classify the inside dynamics of solutions to integrodifference equations as pushed or pulled fronts. The classical integrodifference equation is a discrete-time continuous-space equation that describes a populations growth and spread. The discrete-time aspect coincides with the assumption that the population has nonoverlapping generations. This provides a widely used biological model for population dynamics (Lewis et al. 2016).

2 Mathematical Preliminaries and Model

In this section, we provide necessary background material for the reader. We first discuss the basic model structure with the types of growth functions and dispersal kernels considered in this work. A few integral transforms are then defined for use in the long time analysis of the model. Next, the concept of inside dynamics is then introduced, and the model is formulated. To complete this section, we discuss some classical results for traveling wave solutions and define pushed and pulled traveling wave solutions in terms of the inside dynamics.

2.1 Model Structure

The classical integrodifference equation, describing the growth and dispersal of a population density u, is given by

$$u_{t+1}(x) = \int_{-\infty}^{\infty} k(x - y)g(u_t(y))u_t(y) \, dy. \tag{1}$$

In Eq. (1), g is the density-dependent per capita growth rate function describing the local growth of the population at location y and time t. We assume that g is a non-negative continuous function where $g(u)u$ has a trivial steady state and a steady state at 1. The function k is a probability density function that describes the probability of movement of individuals from location y to location x. That is, k is a nonnegative function that integrates to one. The recursion in Eq. (1) describes the reproduction and dispersal of a population with nonoverlapping generations. That is, all individuals first undergo reproduction and then the offspring are redistributed before reproduction
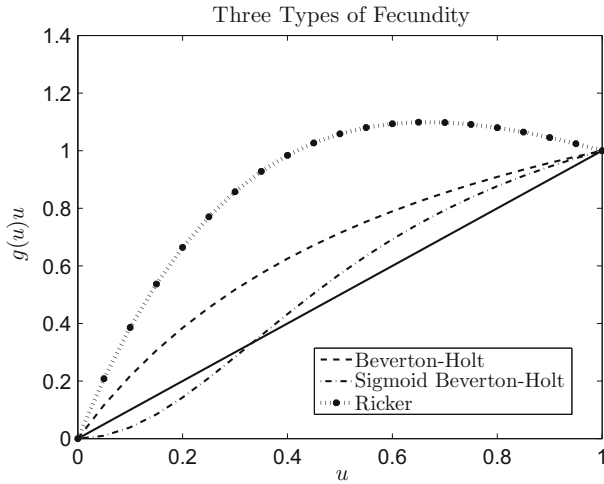
Fig. 1 Fecundity functions, $g(u)u$, used in the numerical simulations. The intrinsic growth rate, R, for the Beverton–Holt, Sigmoid Beverton–Holt, and Ricker type growth functions are 2.5, 4, and 1.5, respectively. The positive sigmoid scaling parameter, δ, for the Sigmoid Beverton–Holt function is chosen to be 2. The *solid line* is the reference line $g(u)u = u$ dictating when there is no change in population density

occurs in the next generation. Given an initial condition $u_0(x)$, $u_t(x)$ is the solution to Eq. (1) defined recursively.

For the population growth, we consider three different types of functions that include different kinds of effects. In particular, we look at Beverton–Holt, Ricker, and Sigmoid Beverton–Holt type growth functions, see Fig. 1.

The classical Beverton–Holt growth is the discrete analog of logistic growth, and the per capita growth is defined by

$$g_{\mathrm{bh}}(u) = \frac{R}{1 + (R - 1)u}, \tag{2}$$

where R is the geometric growth rate. A model introduced by Grant Thompson for fisheries, called the Sigmoid Beverton–Holt model, has per capita growth rate

$$g_s(u) = \frac{Ru^{\delta-1}}{1 + (R - 1)u^\delta}, \tag{3}$$

where R is the intrinsic growth rate and δ is a positive sigmoid scaling parameter (Thompson 1993). It is known that when $\delta > 1$ this growth function exhibits a strong Allee effect.

Since we have scalar discrete-time equations we can consider growth functions with overcompensation. This is not possible for a scalar first order continuous-time model. Ricker type growth is commonly used when overcompensation is present. The Ricker model has the form

$$g_r(u) = e^{R(1-u)}, \tag{4}$$

where R is the intrinsic growth rate (Ricker 1954). Note that $g_{\mathrm{bh}}(u)u$ and $g_s(u)u$ are monotone where $g_r(u)u$ is not, see Fig. 1.

Definition 1 (*Thin-tailed dispersal kernel*) A dispersal kernel $k(x)$ is called *thin-tailed* if there exists a real valued $\xi > 0$, such that

$$\int_{-\infty}^{\infty} k(x)e^{\xi|x|}\,\mathrm{d}x < \infty. \tag{5}$$

If a dispersal kernel is not thin-tailed, then we say the dispersal kernel is *fat-tailed*. For simplicity, we only consider thin-tailed dispersal kernels in this work. Many of the classical mathematical results for the dynamics of Eq. (1) focus on thin-tailed dispersal kernels. The thin-tailed assumption implies that $k(x)$ decays at least as fast as an exponential function as $|x| \to \infty$. A consequence of the thin-tailed assumption is that k has a moment generating function. A common dispersal kernel that we consider throughout our work is the Gaussian probability distribution function. That is:

$$k(x) = \frac{1}{\sqrt{2\pi\sigma^2}}e^{-\frac{(x-\mu)^2}{2\sigma^2}}, \tag{6}$$

where μ is the mean shift in location and σ^2 is the variance in dispersal distance. In the following sections, we use the shorthand notation k is $N(\mu, \sigma^2)$.

2.2 Integral Transforms

The two integral transforms that are particularly useful in our work are the Fourier transform and the reflected bilateral Laplace transform (Zemanian 1968). These transformations and their inverses are given in Definitions 2 and 3.

Definition 2 (*Fourier transform*) Let $f : \mathbb{R} \to \mathbb{R}$ where $f \in L^1(\mathbb{R})$. Then, the Fourier transform and its inverse are, respectively, defined to be

$$\hat{f}(\omega) = \mathcal{F}[f(x)] = \int_{-\infty}^{\infty} f(x)e^{-i\omega x}\,\mathrm{d}x, \text{ and} \tag{7}$$

$$f(x) = \mathcal{F}^{-1}[\hat{f}(\omega)] = \frac{1}{2\pi}\int_{-\infty}^{\infty} \hat{f}(\omega)e^{i\omega x}\,\mathrm{d}\omega. \tag{8}$$

Definition 3 (*Reflected bilateral Laplace transform*) Let $f : \mathbb{R} \to \mathbb{R}$ where f is piecewise continuous on every finite interval in $\mathbb{R}$ satisfying $|f(x)| \leq Me^{-sx}$ for all $x \in \mathbb{R}$ and $0 < s < s_{max}$. Then, the reflected bilateral Laplace transform and its inverse are, respectively, defined to be

$$F(s) = \mathcal{M}[f(x)] = \int_{-\infty}^{\infty} f(x)e^{sx}\,\mathrm{d}x, \text{ and} \tag{9}$$

$$f(x) = \mathcal{M}^{-1}[F(s)] = \frac{1}{2\pi i}\lim_{R\to\infty}\int_{\gamma-iR}^{\gamma+iR} F(s)e^{-sx}\,\mathrm{d}s \tag{10}$$

for $0 < s < s_{\max}$, where the integration in Eq. (10) is over the vertical line, $\text{Re}(s) = \gamma$ in the complex plane and γ is greater than the real parts of all singularities of $F(s)$.

The reflected bilateral Laplace transform can be used to write the solution to our model in terms of its initial condition by using the convolution theorem. This theorem states that the reflected bilateral Laplace transform of a convolution is the product of the reflected bilateral Laplace transforms. That is,

$$\mathcal{M}[f(x) * h(x)](s) = F(s)H(s). \tag{11}$$

Note that the reflected bilateral Laplace transform of a probability density function is also referred to as its moment generating function (Casella and Berger 2002).

2.3 Inside Dynamics

To include neutral genetic diversity, we assume that the population density is composed of either haploid individuals or genes. To analyze the inside dynamics, we separate the population into different neutral fractions $v_t^i(x)$. The initial population is defined to be

$$u_0(x) := \sum_{i=1}^{N} v_0^i(x), \tag{12}$$

where $v_0^i(x) \geq 0$ is the initial population density for neutral fraction i and N is the finite number of distinct neutral fractions. We assume that the individuals (or genes) in each fraction have the same dispersal and growth capabilities as the entire population u and only differ by position and their label (or their alleles). In short, we assume that individuals in each neutral fraction have no genetic advantage over any other neutral fraction. Then, by decomposing the population density into the neutral fractions gives the following system of N equations:

$$v_{t+1}^i(x) = \int_{-\infty}^{\infty} k(x - y)g(u_t(y))v_t^i(y)\, dy, \tag{13}$$

where g is the common per capita growth rate for all neutral fractions. That is, the per capita growth rate of each neutral fraction is the same as the per capita growth rate of the total population giving no genetic advantage of one fraction over another. A key feature of System (13) is that the sum of the neutral fraction densities, $v_t^i(x)$, is equal to the entire population density $u_t(x)$. When we add together the N equations in System (13), we obtain the integrodifference equation for the entire population density given by Eq. (1). Using System (13), we are now able to track how individual neutral fractions spread.

2.4 Traveling Wave Solutions

We focus our study on classifying the traveling wave solutions of Eq. (1). A traveling wave solution $U(x - ct)$ is a solution that connects the trivial steady state, 0, to

the stable nontrivial steady state, 1, and propagates at a constant speed c. That is $u_t(x) = U(x - ct)$ solves equation (1) with constant density profile U. The traveling wave equation is given by

$$U(x - c) = \int_{-\infty}^{\infty} k(x - y)g(U(y))U(y)\,\mathrm{d}y. \tag{14}$$

Weinberger was a pioneer in this area and created the seminal work that analyzed traveling wave solutions for scalar discrete-time operators (Weinberger 1982). The main result in his work shows that for thin-tailed dispersal kernels, if $g(u)u$ is nondecreasing, then Eq. (1) has a family of monotone traveling wave solutions parameterized by the speed c where $c \geq c^*$. The asymptotic spreading speed, c^*, is defined to be the asymptotic speed that a wave with compact initial conditions spreads. It was later shown that the asymptotic spreading speed is the minimum speed for which traveling wave solutions exist. In addition, if the per capita growth rate is maximal at zero, $g(u) \leq g(0)$, then the asymptotic spreading speed can be determined by a simple formula involving $g(0)$ and the dispersal kernel $k(x)$ given below

$$c^* = \inf_{z>0} \frac{1}{z} \ln \left(g(0) \int_{-\infty}^{\infty} k(x)\mathrm{e}^{zx}\,\mathrm{d}x \right). \tag{15}$$

For Gaussian dispersal kernels, we can write down an explicit formula for the asymptotic spreading speed

$$c^* = \sqrt{2\sigma^2 \ln(g(0))} + \mu. \tag{16}$$

Many of the fundamental techniques and concepts presented by Weinberger such as the comparison principle, asymptotic spreading speed, and integral transforms will be used in our analysis.

Weinberger's results were extended to include growth functions that have overcompensatory dynamics (Li et al. 2009). The extended theory requires some additional assumptions on the growth function, but commonly used functions such as the Ricker or logistic growth functions satisfy the required assumptions. In this scenario, it is not guaranteed that the traveling wave profile is monotone. The effect of overcompensation allows for complicated or even chaotic dynamics. Existence of traveling wave solutions with a strong Allee effect has been proven for a unique speed $c = c^*$ (Lui 1983). The decay of the wave profile is given by $U(x) \sim C\mathrm{e}^{-s^*x}$ as $x \to \infty$ where s^* is the unique positive root of

$$\frac{1}{s} \ln \left(g(0) \int_{-\infty}^{\infty} \mathrm{e}^{sx}k(x)\,\mathrm{d}x \right) = c, \tag{17}$$

see Proposition 5 of Lui (1983). In the case where k is $N(\mu, \sigma^2)$ we can explicitly calculate s^* to be

$$s^* = \frac{c - \mu + \sqrt{(\mu - c)^2 - 2\sigma^2 \ln(g(0))}}{\sigma^2}. \tag{18}$$

Thus, we can conclude that $e^{\frac{c-\mu}{\sigma^2}x}U(x) \in L^1(\mathbb{R})$. When Eq. (1) has a strong Allee effect, there are still many open questions. In our work, we conjecture about the decay rate of pushed fronts that comes from the proof for growth functions with a strong Allee effect.

The techniques used to prove results for strong Allee are based on functional analysis arguments for superpositive operators. A linear operator is called *superpositive* (Krasnosel'skii and Zabreiko 1984) if it has a simple positive dominant eigenvalue with positive eigenfunction where no other eigenfunction is positive. In particular, Jentsch's theorem provides sufficient conditions for a linear integral operator to be superpositive (Vladimirov 1971).

In this paper, we focus on pulled and pushed fronts; see Definitions 4 and 5 for details. Instead of using the classical definitions of pulled and pushed fronts (Stokes 1976; Rothe 1981) we classify the waves using the asymptotic dynamics of the neutral fractions. The following definitions come from the previous work on inside dynamics (Bonnefon et al. 2014).

Definition 4 (*Pulled front*) A traveling wave solution $u_t(x) = U(x - ct)$ is said to be a pulled front if, for any neutral fraction $v_t^i(x)$ satisfying (13), $0 \leq v_0^i \leq U$ and $v_0^i(x) = 0$ for large x, the statement

$$v_t^i(x + ct) \to 0 \text{ as } t \to \infty,$$

holds uniformly on any compact subset of $\mathbb{R}$.

Next, we define what it means for a traveling wave solution to be a pushed front in terms of the neutral fractions.

Definition 5 (*Pushed front*) A traveling wave solution $u_t(x) = U(x - ct)$ is said to be a pushed front if, for any neutral fraction $v_t^i(x)$ satisfying (13), $0 \leq v_0^i \leq U$ and $v_0^i \not\equiv 0$, there exists $M > 0$ such that

$$\limsup_{t \to \infty} \sup_{x \in [-M, M]} v_t^i(x + ct) > 0.$$

To recap, the preliminary definitions, theory, techniques, and the mathematical model have been laid out. Now that we have all the required knowledge we move into the next section where we classify the asymptotic dynamics of System (13).

3 Large Time Neutral Genetic Variation

In this section, we provide the theoretical results about the neutral genetic composition for System (13). In Theorems 1 and 2, we assume that the dispersal kernel is Gaussian,

see Eq. (6). This allows us to exploit the fact that the moment generating function for a Gaussian has the following form:

$$M(s) = e^{\mu s + \sigma^2 s^2 / 2}. \tag{19}$$

After the proof of Theorem 1, we provide two corollaries that provide a better interpretation for the results of Theorem 1. We then extend the results of Theorem 1 to the general class of thin-tailed dispersal kernels given by Theorem 3.

Theorem 1 (Gaussian kernel with maximum per capita growth at zero) *Consider the solution of System* (12)–(13) *where k is* $N(\mu, \sigma^2)$ *and* $0 < g(u) \le g(0)$ *for all u* $\in$ (0, 1). *Let c be the speed of a moving half-frame. If* $c \ge c^*$ *and* $\int_{-\infty}^{\infty} e^{\frac{c-\mu}{\sigma^2} y} v_0^i(y) \, dy < \infty$, *then for any* $A \in \mathbb{R}$, *the density of the neutral fraction i,* $v_t^i(x)$, *converges to 0 uniformly as* $t \to \infty$ *in the moving half-frame* $[A + ct, \infty)$.

Proof For simplicity in notation, we focus on a single neutral fraction and drop the superscript i notation. Using the fact that $0 < g(u) \le g(0)$ for all $u \in (0, 1)$, we can use a comparison principle to show that a new sequence $w_t(x)$ defined by

$$w_{t+1}(x) = g(0) \int_{-\infty}^{\infty} k(x - y) w_t(y) \, dy \tag{20}$$

is always greater than the solution to any neutral fraction $v_t(x)$ with the same initial condition $w_0(x) = v_0(x)$. The solution of Eq. (20) is given by the t-fold convolution

$$w_t(x) = (g(0))^t k^{*t} * w_0(x) \tag{21}$$

where k^{*t} is k convolved with itself t times. Applying the reflected bilateral Laplace transform to Eq. (21) and using the convolution theorem, we obtain

$$\mathcal{M}[w_t(x)](s) = [g(0)]^t \left[\mathcal{M}[k(x)](s) \right]^t \mathcal{M}[w_0(x)](s) \tag{22}$$

$$= [g(0)]^t \left[e^{\frac{\sigma^2 s^2}{2} + \mu s} \right]^t \mathcal{M}[w_0(x)](s) \tag{23}$$

$$= [g(0)]^t e^{\frac{\sigma^2 t s^2}{2} + \mu t s} \mathcal{M}[w_0(x)](s) \tag{24}$$

$$= [g(0)]^t \mathcal{M} \left[\frac{1}{\sqrt{2\pi\sigma^2 t}} e^{-\frac{(x-\mu t)^2}{2\sigma^2 t}} \right] (s) \mathcal{M}[w_0(x)](s) \tag{25}$$

$$= [g(0)]^t \mathcal{M}[k_t * w_0)(x)](s), \tag{26}$$

where k_t is $N(\mu t, \sigma^2 t)$. Then applying the inverse transform yields

$$w_t(x) = [g(0)]^t (k_t * w_0)(x) \tag{27}$$

$$= [g(0)]^t \int_{-\infty}^{\infty} \frac{1}{\sqrt{2\pi\sigma^2 t}} e^{-\frac{(x-y-\mu t)^2}{2\sigma^2 t}} w_0(y) \, dy. \tag{28}$$

In the moving half-frame $[A + ct, \infty)$ with fixed $A \in \mathbb{R}$, consider the element $x_0 + ct$ with $c \geq c^* = \sqrt{2\sigma^2 \ln(g(0))} + \mu$. When we rewrite $w_t(x)$ in this moving half-frame we have

$$w_t(x_0 + ct) = [g(0)]^t \int_{-\infty}^{\infty} \frac{1}{\sqrt{2\pi\sigma^2 t}} e^{-\frac{(x_0+ct-y-\mu t)^2}{2\sigma^2 t}} w_0(y) \, dy. \qquad (29)$$

Expanding the exponent, yields

$$\frac{(x_0 + ct - y - \mu t)^2}{2\sigma^2 t} = \frac{(x_0 - y)^2}{2\sigma^2 t} + \frac{2(c - \mu)t(x_0 - y) + (c - \mu)^2 t^2}{2\sigma^2 t} \qquad (30)$$

$$\geq \frac{(x_0 - y)^2}{2\sigma^2 t} + \frac{c - \mu}{\sigma^2}(x_0 - y) + \ln(g(0))t. \qquad (31)$$

Thus,

$$w_t(x_0 + ct) \leq \frac{e^{\ln(g(0))t}}{\sqrt{2\pi\sigma^2 t}} \int_{-\infty}^{\infty} e^{-\frac{(x_0-y)^2}{2\sigma^2 t}} e^{-\frac{c-\mu}{\sigma^2}(x_0-y)} e^{-\ln(g(0))t} w_0(y) \, dy \qquad (32)$$

$$= \frac{1}{\sqrt{2\pi\sigma^2 t}} \int_{-\infty}^{\infty} e^{-\frac{(x_0-y)^2}{2\sigma^2 t}} e^{-\frac{c-\mu}{\sigma^2}(x_0-y)} w_0(y) \, dy \qquad (33)$$

$$= \frac{e^{-\frac{c-\mu}{\sigma^2} x_0}}{\sqrt{2\pi\sigma^2 t}} \int_{-\infty}^{\infty} e^{-\frac{(x_0-y)^2}{2\sigma^2 t}} e^{\frac{c-\mu}{\sigma^2} y} w_0(y) \, dy. \qquad (34)$$

Since $x_0 \geq A$ we have

$$w_t(x_0 + ct) \leq \frac{e^{-\frac{A(c-\mu)}{\sigma^2}}}{\sqrt{2\pi\sigma^2 t}} \int_{-\infty}^{\infty} e^{\frac{c-\mu}{\sigma^2} y} w_0(y) \, dy. \qquad (35)$$

Thus since $\int_{-\infty}^{\infty} e^{\frac{c-\mu}{\sigma^2} y} w_0(y) \, dy < \infty$ we have $w_t(x_0 + ct) \to 0$ uniformly as $t \to \infty$ in $[A, \infty)$. Recall that $w_t(x)$ was constructed so that $0 \leq v_t(x) \leq w_t(x)$. This implies the uniform convergence of $v_t(x) \to 0$ as $t \to \infty$ in the moving half-frame $[A + ct, \infty)$. $\qquad \square$

Corollary 1 (Compact initial conditions) *Consider the solution of System* (12)–(13) *where k is $N(\mu, \sigma^2)$ and $0 < g(u) \leq g(0)$ for all $u \in (0, 1)$ with compactly supported initial conditions $v_0^i(x)$ for $i = 1, \ldots, N$. Then each neutral fraction converges to zero uniformly to zero as $t \to \infty$ in the moving half-frame $[A + ct, \infty)$ where $c \geq c^*$.*

This result is clear from the condition that any compact initial conditions will satisfy the assumption of Theorem 1 that $\int_{-\infty}^{\infty} e^{\frac{c-\mu}{\sigma^2} y} v_0^i(y) \, dy < \infty$. This result is relevant because when we perform numerical simulations we must use compact initial conditions. Thus, it takes time for the traveling wave solution to spread at the asymptotic spreading speed c^*. Therefore, we will always outrun the solution by looking in the moving half-frame $[A + c^*t, \infty)$.

For the next corollary, we consider initial conditions were $u_0(x) = \sum_{i=1}^{N} v_0^i(x) = U(x)$ and $v_0^1(x) = \mathbb{1}_{x \geq a} U(x)$ where a is a constant. Here, we call $v_0^1(x)$ the neutral fraction at the leading edge of the traveling wave.

Corollary 2 (Traveling wave initial conditions) *Consider the solution of System* (12)–(13) *where k is* $N(\mu, \sigma^2)$ *and* $0 < g(u) \leq g(0)$ *for all* $u \in (0, 1)$ *with initial condition* $\sum_{i=1}^{N} v_0^i(x) = U(x)$ *with speed* $c \geq c^*$. *Then the neutral fraction at the leading edge of the traveling wave converges to* $U(x)$ *uniformly as* $t \to \infty$ *in the moving half-frame* $[A + ct, \infty)$ *and all other neutral fractions converges to zero uniformly to zero as* $t \to \infty$ *in the moving half-frame* $[A + ct, \infty)$.

In Corollary 2, the initial conditions for System (13) sum to be the traveling wave solution with speed greater than or equal to the minimum asymptotic spreading speed c^*. In this case, we know that traveling wave solutions exist for all $c \geq c^*$ (Weinberger 1982). The key question is what happens to the neutral fraction at the front of the spread. We see that all other neutral fractions vanish when the moving half-frame is sufficiently far to the right. Thus, each one of these neutral fractions satisfy the assumption $\int_{-\infty}^{\infty} e^{\frac{c-\mu}{\sigma^2} y} v_0^i(y) \, dy < \infty$ required for Theorem 1. However, the neutral fraction at the leading edge decays no faster than $e^{-\frac{c-\mu}{\sigma^2} y}$. Thus, $\int_{-\infty}^{\infty} e^{\frac{c-\mu}{\sigma^2} y} v_0^i(y) \, dy$ is not finite, and hence, one cannot apply Theorem 1 to this neutral fraction. However, if all other neutral fractions approach zero then it must be the case that the neutral fraction at the leading edge of the traveling wave converges to U uniformly as $t \to \infty$ in the moving half-frame $[A + ct, \infty)$. From Definition 4, it is clear that the results from Corollary 2 show that the solution to System (12)–(13) where k is $N(\mu, \sigma^2)$, $0 < g(u) \leq g(0)$ for all $u \in (0, 1)$, and $\sum_{i=1}^{N} v_0^i(x) = U(x)$ is a pulled front.

Next, we extend the theory to consider growth functions with a strong Allee effect. The idea of proof is different from Theorem 1 because we can no longer construct a supersolution by using the linearization. Instead, we use Hilbert-Schmidt theory to obtain the asymptotic dynamics.

Theorem 2 (Gaussian kernel with strong Allee type growth) *Consider the solution of System* (12)–(13) *where k is* $N(\mu, \sigma^2)$, *g has a strong Allee effect, and* $\sum_{i=1}^{N} v_0^i(x) = U(x)$. *Then for any* $A \in \mathbb{R}$, *the density of neutral fraction i,* $v_t^i(x)$, *converges to a proportion* $p^i[v_0^i]$ *of the total population* $U(x - ct)$ *uniformly as* $t \to \infty$ *in the moving half-frame* $[A + ct, \infty)$. *That is,* $\left| v_t^i(x) - p^i[v_0^i] U(x - ct) \right| \to 0$ *uniformly as* $t \to \infty$ *in the moving half-frame* $[A + ct, \infty)$. *Moreover, if* $e^{\frac{c-\mu}{\sigma^2} x} U(x) \in L^2(\mathbb{R})$, *then the proportion* $p^i[v_0^i]$ *can be computed explicitly:*

$$p^i[v_0^i] = \frac{\int_{-\infty}^{\infty} v_0^i(x) U(x) e^{\frac{c-\mu}{\sigma^2/2} x} \, dx}{\int_{-\infty}^{\infty} U^2(x) e^{\frac{c-\mu}{\sigma^2/2} x} \, dx}. \tag{36}$$

Proof Consider System (13) where k is $N(\mu, \sigma^2)$ and g has a strong Allee effect. For simplicity in notation, we focus on a single neutral fraction and drop the superscript i notation. Define $\tilde{v}_t(x) = v_t(x + ct)$, then

$$\tilde{v}_{t+1}(x) = \int_{-\infty}^{\infty} k(x+c-y)g(U(y))\tilde{v}_t(y)\,\mathrm{d}y. \tag{37}$$

Since k is $N(\mu, \sigma^2)$,

$$k(x+c-y) = \frac{1}{\sqrt{2\pi\sigma^2}}e^{-\frac{(x+c-y-\mu)^2}{2\sigma^2}} \tag{38}$$

$$= \frac{1}{\sqrt{2\pi\sigma^2}}e^{-\frac{(x-y)^2}{2\sigma^2}}e^{-\frac{(c-\mu)^2}{2\sigma^2}}e^{-\frac{c-\mu}{\sigma^2}x}e^{\frac{c-\mu}{\sigma^2}y} \tag{39}$$

$$= \tilde{k}(x-y)e^{-\frac{(c-\mu)^2}{2\sigma^2}}e^{-\frac{c-\mu}{\sigma^2}x}e^{\frac{(c-\mu)}{\sigma^2}y} \tag{40}$$

where $\tilde{k}$ is $N(0, \sigma^2)$. Define $v_t^*(x) = e^{\frac{c-\mu}{\sigma^2}x}\tilde{v}_t(x)$. Then Eq. (37) becomes

$$v_{t+1}^*(x) = \int_{-\infty}^{\infty} e^{-\frac{(c-\mu)^2}{2\sigma^2}}\tilde{k}(x-y)g(U(y))v_t^*(y)\,\mathrm{d}y. \tag{41}$$

We know that the weight function $\rho(y) = e^{-\frac{(c-\mu)^2}{2\sigma^2}}g(U(y))$ is a positive and continuous function and $\rho(y)\tilde{k}(x-y) \in L^2(\mathbb{R})$. Then we consider

$$\phi(x) = \int_{-\infty}^{\infty} e^{-\frac{c-\mu}{2\sigma^2}}\tilde{k}(x-y)g(U(y))\phi(y)\,\mathrm{d}y. \tag{42}$$

Multiplying equation (42) on both sides by $\sqrt{\rho(x)}$, we have

$$\sqrt{\rho(x)}\phi(x) = \int_{-\infty}^{\infty} \sqrt{\rho(x)}\tilde{k}(x-y)\sqrt{\rho(y)}\sqrt{\rho(y)}\phi(y)\,\mathrm{d}y. \tag{43}$$

Since $\tilde{k}$ is $N(0, \sigma^2)$, the function $\bar{k}(x, y) := \sqrt{\rho(x)}\tilde{k}(x-y)\sqrt{\rho(y)}$ is symmetric; $\bar{k}(x, y) = \bar{k}(y, x)$. Therefore, the Hilbert–Schmidt theory can still be applied with a nonsymmetric kernel. Also $\phi(x) = e^{\frac{c-\mu}{\sigma^2}x}U(x)$ is a positive eigenfunction of Eq. (42) with eigenvalue 1. Thus, by Jentsch's theorem (Vladimirov 1971), since our eigenfunction is positive, this eigenfunction is associated with the eigenvalue with the largest modulus. Therefore, we know that all other eigenvalues have modulus strictly less than one. We can write the solution by eigenfunction expansion as

$$v_t^*(x) = p\phi(x) + z_t(x) \tag{44}$$

where p is a scalar and $z_t(x)$ is composed of elements that are orthogonal to $\phi(x)$ for each $t \in \mathbb{N}$ and $|z_t(x)| \le K|\lambda|^t$ for some constants $K > 0$ and $|\lambda| < 1$. Hence,

$$\left|v_t^*(x) - p\phi(x)\right| \le K|\lambda|^t. \tag{45}$$

Converting back to the moving frame coordinates,

$$\left| e^{\frac{c-\mu}{\sigma^2}x} \tilde{v}_t(x) - p e^{\frac{c-\mu}{\sigma^2}x} U(x) \right| \le K |\lambda|^t . \tag{46}$$

Thus,

$$|\tilde{v}_t(x) - pU(x)| \le K e^{-\frac{c-\mu}{\sigma^2}x} |\lambda|^t . \tag{47}$$

From this, we can conclude that $|\tilde{v}_t(x) - pU(x)| \to 0$ uniformly as $t \to \infty$ in the interval $[A, \infty)$. Therefore, $|v_t(x) - pU(x - ct)| \to 0$ uniformly as $t \to \infty$ in the moving half-frame $[A + ct, \infty)$.

To obtain the proportion p, we multiply equation (44) evaluated at $t = 0$ by $\phi(x)$ and integrate to obtain

$$\int_{-\infty}^{\infty} v_0^*(x)\phi(x)\, dx = \int_{-\infty}^{\infty} p\phi^2(x)\, dx + \int_{-\infty}^{\infty} z_0(x)\phi(x)\, dx \tag{48}$$

$$= p \int_{-\infty}^{\infty} \phi^2(x)\, dx \tag{49}$$

by the orthogonality of z to ϕ. Solving for p we find

$$p = \frac{\int_{-\infty}^{\infty} v_0^*(x)\phi(x)\, dx}{\int_{-\infty}^{\infty} \phi^2(x)\, dx} \tag{50}$$

$$= \frac{\int_{-\infty}^{\infty} e^{\frac{c-\mu}{\sigma^2}x} \tilde{v}_0(x) e^{\frac{c-\mu}{\sigma^2}x} U(x)\, dx}{\int_{-\infty}^{\infty} \left(e^{\frac{c-\mu}{\sigma^2}x} U(x) \right)^2 dx} \tag{51}$$

$$= \frac{\int_{-\infty}^{\infty} v_0(x) U(x) e^{\frac{c-\mu}{\sigma^2/2}x}\, dx}{\int_{-\infty}^{\infty} U^2(x) e^{\frac{c-\mu}{\sigma^2/2}x}\, dx}. \tag{52}$$

The proof of Theorem 2 is complete.   □

From Definition 5, it is clear that the results from Theorem 2 show that the solution to System (12)–(13) where k is $N(\mu, \sigma^2)$, g has a strong Allee effect, and $u_0(x) = U(x)$ is a pushed front.

The next step in our work is to extend the result of Theorem 1 to a general class of thin-tailed dispersal kernels. To accomplish this goal, we must place some extra constraints on the initial conditions for the neutral fractions. That is, we define the set $B_s := \{v_0^i : x^2 v_0^i(x) e^{sx} \in L^1(\mathbb{R}) \cap L^\infty(\mathbb{R})\}$. This condition is given as the assumption of Lemma 1.

Lemma 1 *Let $v_0^i(x) \in B_s$ for all $s > 0$, then there exists a positive constant C such that*

$$w_0^i(x) := \frac{Ce^{-sx}}{1+x^2} \tag{53}$$

bounds $v_0^i(x)$ for all $x \in \mathbb{R}$. Moreover, the Fourier transform of $w_0^i(x)e^{sx}$ with respect to x is in $L^1(\mathbb{R})$ and is given by

$$C\pi e^{-|\omega|}. \tag{54}$$

The proof of Lemma 1 is provided in the section "Proof of Lemma 1" of the Appendix. Lemma 1 provides important assumptions to guarantee that the initial conditions can be bounded by a function that has a Fourier transform in $L^1(\mathbb{R})$. This result allows us to extend the result of Theorem 1 to a general class of thin-tailed dispersal kernels.

Theorem 3 (Thin-tailed kernel with maximum per capita growth at zero) *Consider the solution of System (12)–(13) where k is a thin-tailed dispersal kernel and g is the per capita growth rate that satisfies $0 < g(u) \leq g(0)$ for all $u \in (0, 1)$. Let c be the speed of a moving half-frame. If $c \geq c^*$ and $v_0^i(x) \in B_{s_0(c)}$ where $s_0(c)$ is the smallest positive root of $\ln(g(0)K(s)) = sc$, then for any $A \in \mathbb{R}$, the density of the neutral fraction i, $v_t^i(x)$, converges to 0 uniformly as $t \to \infty$ in the moving half-frame $[A + ct, \infty)$.*

Proof Consider the neutral fraction model given by System (13). For simplicity, we consider a single neutral fraction $v_t^i(x)$ and drop the superscript i notation. That is,

$$v_t(x) = \int_{-\infty}^{\infty} k(x - y)g(u_{t-1}(y))v_{t-1}(y)\, dy. \tag{55}$$

Equation (1) produces traveling wave solutions $u_t(x) = U(x - ct)$. In the case where k, is a thin-tailed dispersal kernel and $0 < g(u) \leq g(0)$ for all $u \in (0, 1)$ we know that the asymptotic spreading speed c^* can be calculated by

$$c^* = \inf_{s>0} \frac{1}{s} \ln(g(0)K(s)) \tag{56}$$

where $K(s) = \int_{-\infty}^{\infty} k(x)e^{sx}\, dx$ is the moment generating function for the dispersal kernel k. The function $\ln(g(0)K(s))/s$ is positive and convex where $K(s)$ is finite. Thus, there is a unique minimum for c^* obtained at some s^*. That is, $\ln(g(0)K(s^*)) = s^*c^*$. For all $c > c^*$, the equation $\ln(g(0)K(s)) = sc$ has at most two positive roots. We define the smallest positive root by $s_0(c) < s^*$. Using the fact that the per capita growth rate is the largest at zero, we obtain a supersolution $w_t(x)$ to System (55). That is, $w_t(x)$ satisfies the Cauchy problem

$$\begin{cases} w_t(x) = g(0) \int_{-\infty}^{\infty} k(x - y)w_{t-1}(y)\, dy, & t \in \mathbb{N},\ x \in \mathbb{R} \\ w_0(x) = \frac{Ce^{-s_0(c)x}}{1+x^2} \geq v_0(x), & x \in \mathbb{R} \end{cases} \tag{57}$$

where $v_t(x) \leq w_t(x)$ for all $t \geq 0$. The solution of Eq. (57) is given by the t-fold convolution

$$w_t(x) = (g(0))^t k^{*t} * w_0(x). \tag{58}$$

Next, we introduce the reflected bilateral Laplace transform defined in Eq. (9) for all $0 < s < s_{\max}$. It is clear that we can apply this transform to $w_t(x)$ because k is thin-tailed and $w_0(x)$ is defined by Eq. (53). Applying this transform to Eq. (58) and using the convolution property we obtain

$$\mathcal{M}[w_t(x)](s) = (g(0))^t (\mathcal{M}[k(x)](s))^t \mathcal{M}[w_0(x)](s) \tag{59}$$
$$= (g(0))^t (K(s))^t W_0(s). \tag{60}$$

To obtain our solution for $w_t(x)$, we must use the inverse transform, as defined in Eq. (10), given by

$$w_t(x) = \frac{1}{2\pi i} \lim_{R \to \infty} \int_{s_0(c)-iR}^{s_0(c)+iR} (g(0))^t (K(s))^t W_0(s) e^{-sx} \, ds \tag{61}$$

where $0 < \mathrm{Re}(s) < s_{\max}$ is the region of convergence for $(K(s))^t W_0(s) e^{-sx}$. By performing a change of variables to integrate over the real line by letting $s = s_0(c) + i\omega$, we obtain

$$w_t(x) = \frac{1}{2\pi} \int_{-\infty}^{\infty} (g(0))^t (K(s_0(c) + i\omega))^t W_0(s_0(c) + i\omega) e^{-(s_0(c)+i\omega)x} \, d\omega \tag{62}$$

$$= \frac{1}{2\pi} \int_{-\infty}^{\infty} e^{(\mathrm{Log}(g(0))) + \mathrm{Log}(K(s_0(c)+i\omega))t} W_0(s_0(c) + i\omega) e^{-(s_0(c)+i\omega)x} \, d\omega, \tag{63}$$

where Log is the principal value of the complex logarithm. In the moving frame, $x = x_0 + ct$ where $x_0 \in \mathbb{R}$, the solution satisfies

$$w_t(x_0 + ct) = \frac{1}{2\pi} \int_{-\infty}^{\infty} e^{J(s_0(c)+i\omega)t} W_0(s_0(c) + i\omega) e^{-(s_0(c)+i\omega)x_0} \, d\omega, \tag{64}$$

where J is a complex-valued function defined as follows

$$J(s_0(c) + i\omega) := \mathrm{Log}(g(0)) + \mathrm{Log}(K(s_0(c) + i\omega)) - c(s_0(c) + i\omega). \tag{65}$$

Although we expect that $w_t(x)$ as a solution to Eq. (58) is real, this fact is not immediately evident from Eq. (64). Therefore, we treat $w_t(x)$ as if it were a complex-valued function. The modulus of the supersolution is

$$|w_t(x_0 + ct)| = \left| \frac{1}{2\pi} \int_{-\infty}^{\infty} e^{J(s_0(c)+i\omega)t} W_0(s_0(c) + i\omega)e^{-(s_0(c)+i\omega)x_0} \, d\omega \right| \tag{66}$$

$$\leq \frac{1}{2\pi} \int_{-\infty}^{\infty} e^{\mathrm{Re}(J(s_0(c)+i\omega))t} \, |W_0(s_0(c) + i\omega))| \, e^{-s_0(c)x_0} \, d\omega. \tag{67}$$

Using the results from Lemma 1, we have that

$$W_0(s_0(c) + i\omega) = \int_{-\infty}^{\infty} w_0(x)e^{(s_0(c)+i\omega)x} \, dx \tag{68}$$

$$= \int_{-\infty}^{\infty} w_0(x)e^{s_0(c)x}e^{i\omega x} \, dx \tag{69}$$

$$= \mathcal{F}\left[w_0(x)e^{s_0(c)x} \right](-\omega) \tag{70}$$

$$= C\pi e^{-|\omega|} \tag{71}$$

for all $\omega \in \mathbb{R}$. Then using Eq. (67) and the previous result, we have

$$|w_t(x_0 + ct)| \leq \frac{1}{2\pi} \int_{-\infty}^{\infty} e^{\mathrm{Re}(J(s_0(c)+i\omega))t} C\pi e^{-|\omega|}e^{-s_0(c)x_0} \, d\omega. \tag{72}$$

Notice that

$$\mathrm{Re}(J(s_0(c) + i\omega)) = \ln(g(0)) + \mathrm{Re}(\mathrm{Log}(K(s_0(c) + i\omega))) - cs_0(c) \tag{73}$$

$$= \ln(g(0)) + \mathrm{Re}\left(\mathrm{Log}\left(\int_{-\infty}^{\infty} k(x)e^{s_0(c)x}e^{i\omega x} \, dx \right) \right) - cs_0(c). \tag{74}$$

Let us define

$$I := \mathrm{Re}\left(\mathrm{Log}\left(\int_{-\infty}^{\infty} k(x)e^{s_0(c)x}e^{i\omega x} \, dx \right) \right). \tag{75}$$

Using Euler's formula, we find that

$$I = \mathrm{Re}\left(\mathrm{Log}\left(\int_{-\infty}^{\infty} k(x)e^{s_0(c)}(\cos(\omega x) + i\sin(\omega x)) \, dx \right) \right) \tag{76}$$

$$= \ln\left(\sqrt{\left(\int_{-\infty}^{\infty} k(x)e^{s_0(c)x}\cos(\omega x) \, dx \right)^2 + \left(\int_{-\infty}^{\infty} k(x)e^{s_0(c)x}\sin(\omega x) \, dx \right)^2} \right). \tag{77}$$

Define $II := \left(\int_{-\infty}^{\infty} k(x)e^{s_0(c)x}\cos(\omega x)\,dx\right)^2 + \left(\int_{-\infty}^{\infty} k(x)e^{s_0(c)x}\sin(\omega x)\,dx\right)^2$. Using Cauchy-Schwarz inequality we find that

$$II < \int_{-\infty}^{\infty} k(x)e^{s_0(c)x}\,dx \int_{-\infty}^{\infty} k(x)e^{s_0(c)x}\cos^2(\omega x)\,dx + \cdots$$

$$\int_{-\infty}^{\infty} k(x)e^{s_0(c)x}\,dx \int_{-\infty}^{\infty} k(x)e^{s_0(c)x}\sin^2(\omega x)\,dx \tag{78}$$

$$= \int_{-\infty}^{\infty} k(x)e^{s_0(c)x}\,dx \int_{-\infty}^{\infty} k(x)e^{s_0(c)x}\left(\cos^2(\omega x) + \sin^2(\omega x)\right)\,dx \tag{79}$$

$$= \left(\int_{-\infty}^{\infty} k(x)e^{s_0(c)x}\,dx\right)^2. \tag{80}$$

Thus,

$$\text{Re}(J(s_0(c)+i\omega)) < \ln(g(0)) + \ln\left(\sqrt{\left(\int_{-\infty}^{\infty} k(x)e^{s_0(c)x}\,dx\right)^2}\right) - cs_0(c) \tag{81}$$

$$= \ln(g(0)) + \ln\left(\int_{-\infty}^{\infty} k(x)e^{s_0(c)x}\,dx\right) - cs_0(c) \tag{82}$$

$$= \ln(g(0)) + \ln\left(K(s_0(c))\right) - cs_0(c) \tag{83}$$

$$= 0 \tag{84}$$

for $\omega \neq 0$. When $\omega = 0$, we have that $\text{Re}(J(s_0(c)+i\omega)) = 0$. Returning to Inequality (72), by the Dominated Convergence theorem, we have

$$\lim_{t\to\infty} |w_t(x_0 + ct)| \leq \lim_{t\to\infty} \frac{1}{2\pi} \int_{-\infty}^{\infty} e^{\text{Re}(J(s_0(c)+i\omega))t} C\pi e^{-|\omega|} e^{-s_0(c)x_0}\,d\omega \tag{85}$$

$$= \frac{Ce^{-s_0(c)x_0}}{2} \int_{-\infty}^{\infty} \lim_{t\to\infty} e^{\text{Re}(J(s_0(c)+i\omega))t} e^{-|\omega|}\,d\omega \tag{86}$$

$$= 0. \tag{87}$$

Thus, for any $A \in \mathbb{R}$

$$\lim_{t\to\infty} \max_{[A,\infty)} w_t(x + ct) = 0. \tag{88}$$

Since w was chosen to be a supersolution of v, we can conclude that

$$\lim_{t\to\infty} \max_{[A,\infty)} v_t(x + ct) = 0. \tag{89}$$

Therefore, we obtain the desired result that for any $A \in \mathbb{R}$, the density $v_t(x)$ of the neutral fraction converges to 0 uniformly as $t \to \infty$ in the moving half-frame $[A + ct, \infty)$. $\qquad\square$

From Definition 4, it is clear that the results from Theorem 3 show that the solution to System (12)–(13) where k is thin-tailed, $0 < g(u) \leq g(0)$ for all $u \in (0, 1)$, and $\sum_{i=1}^{N} v_0^i(x) = U(x)$ is a pulled front.

This section contains the main mathematical results of our work. We showed that when the dispersal kernel is assumed to be Gaussian we showed two main results. When the per capita growth is maximal at zero we see that all neutral fractions converge to zero uniformly in the moving frame. If the growth function has a strong Allee effect, then all neutral fractions contribute to the spread. Moreover, the proportion of each neutral fraction in the spread is given by Eq. (36). We then extended the first result to thin-tailed dispersal kernels showing that when the per capita growth is maximal at zero we see that all neutral fractions converge to zero uniformly in the moving frame.

4 Numerical Simulations

The numerical simulations were performed using MATLAB. To calculate the convolution

$$\int_{-\infty}^{\infty} k(x - y) g(u_t(y)) v_t^i(y) \, \mathrm{d}y \qquad (90)$$

we use a numerical "fast Fourier transform" (`fft`) with inverse (`ifft`). Solving the problem by using the convolution theorem, changes the numerical scheme to become $O(n \log n)$ instead of $O(n^2)$. Numerically, we implement the following strategy

$$k * (g \cdot v^i) = \texttt{ifft}(\texttt{fft}(k) \cdot \texttt{fft}(g \cdot v^i)). \qquad (91)$$

For simplicity, in all the numerical simulations we start with the same initial condition and use the same dispersal kernel. We assume that there are eight neutral fractions in the population and assume that they satisfy $v_0^i(x) = \mathbb{1}_{(-0.5i, -0.5(i-1)]}$ where $\mathbb{1}_S$ is the indicator function on a set S. This assumes that we have the strongest initial spatial heterogeneity between the neutral fractions, see Fig. 2a for a plot of the initial conditions. The dispersal kernel is assumed to be Gaussian with $\mu = 0$ and $\sigma^2 = 0.002$. That is,

$$k(x - y) = \frac{1}{\sqrt{0.004\pi}} \mathrm{e}^{-\frac{(x-y)^2}{0.004}}. \qquad (92)$$

Simulations for System (13) with the different types of growth functions are provided in Fig. 2.

The interpretation of the simulations provided in Fig. 2 must be made carefully because, without proper explanation, they may be misunderstood. In Fig. 2, the light gray component is the sum all eight neutral fractions. The red component is plotted in front of the light gray and is given by the sum of all neutral fractions except the first one. The same process continues for the rest of the six colors yellow, green, light blue, blue, and dark gray, respectively. The easiest way to interpret the numerical results presented in Fig. 2 is by looking at a vertical strip of the solution for a particular value
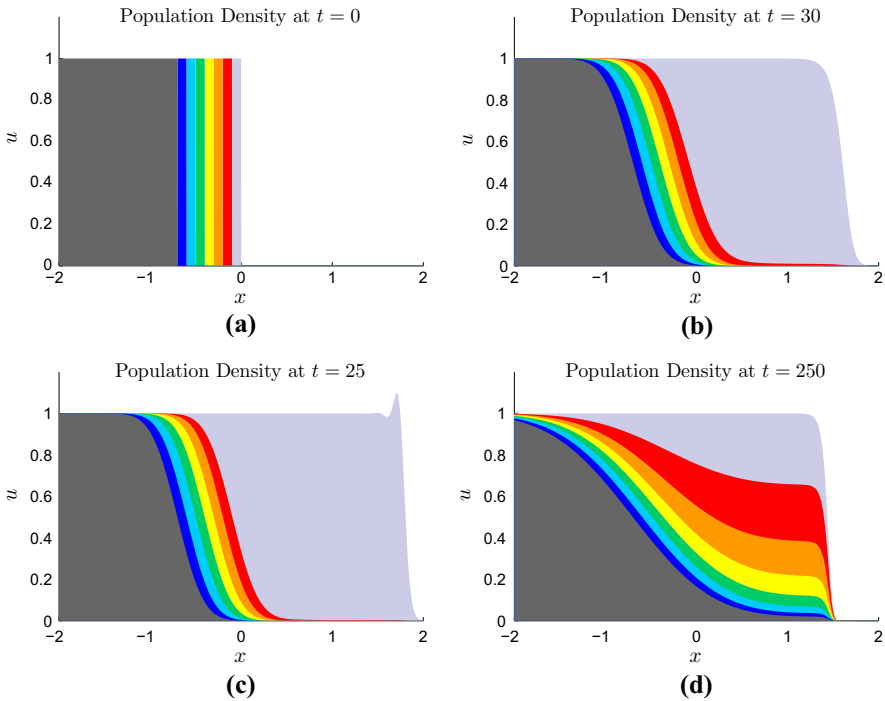
Fig. 2 Numerical realization for the solution $u_t(x)$ of System (13) for three different per capita growth functions. **a** The initial condition for the simulations. **b** Beverton–Holt growth with parameter values $R = 2.5$ at time $t = 30$. **c** Ricker growth with parameter values $R = 1.5$ at time $t = 25$. **d** Sigmoid Beverton–Holt growth with parameter values $R = 4$ and $\delta = 2$ at time $t = 250$ (Color figure online)

of x. From this perspective, the amount of color showing for each neutral fraction dictates the proportion of that fraction to the entire population density at a particular location x. For example, we can see from the initial condition in Fig. 2a that each neutral fraction has complete spatial segregation from other neutral fractions.

In Fig. 2b, we observe that only the rightmost fraction drives the propagation of the total population where as the trailing populations will be left behind in the moving frame. In Fig. 2c, we observe that the leading neutral fraction dominates the spread, but in this case the traveling wave is nonmonotone. In Fig. 2d, the inclusion of a strong Allee effect promotes genetic diversity in the colonization front. The numerical results suggest that the classification of pulled and pushed fronts should be able to be extended for initial conditions other than the traveling wave profile $U(x)$. The complexity in extending the results lie in understanding how to choose the correct speed for the moving half-frame.

It should be noted that the simulations are numerical approximations to System (13) because the domain where we can compute the numerics is finite. The results shown in Fig. 2 provide numerical support for the extension of the results presented in the previous section to compact initial conditions. For Theorem 2 and Corollary 2, the results require that the initial conditions are in the form of the traveling wave

solution $U(x)$. However, since the computational domain is finite, we know that all the initial conditions will have finite support. This means that we obtain the results from Corollary 1 when the per capita growth rate is maximal at zero which states that if we move the frame at speed c^* then asymptotically all neutral fractions approach zero. This is because compact initial conditions that converges to a front moving at speed c^* would have fallen behind the moving half-frame that travels at speed c^* for all time.

5 Discussion

The work presented in this paper develops a mathematical model to understand the role that dispersal into new territory has on the neutral genetic composition of a population with discrete nonoverlapping generations. We construct our model using the integrodifference framework where space is continuous but time is discrete.

This work extends the previous results on the mathematical analysis of inside dynamics to include discrete-time dynamics. All previous analyses of inside dynamics have assumed continuous-time dynamics. By working with discrete-time models, we explore how overcompensation affects the neutral genetic diversity. Since this phenomena is not possible for a scalar continuous-time model, the analysis of the overcompensatory growth is fundamentally new.

We were able to prove asymptotic results about the genetic structure of the expanding population. First, we considered Gaussian dispersal with two different kinds of growth functions. The first having maximum per capita growth at zero, and the second having a strong Allee effect. The results are given by Theorems 1 and 2. The theorems provide very different asymptotic behavior for solutions whose initial conditions are in the shape of the traveling wave solution.

For growth functions whose per capita growth is maximal at zero, we see that the spread of the population is dominated by the leading neutral fraction and all other neutral fractions approach zero, see Corollary 2. However, we are only able to conclude this result when the initial population density is in the shape of the traveling wave solution. Mathematically, this is analogous with the concept of a pulled front where the dynamics of the spread are governed solely by what happens at the leading edge of the wave. From a biological perspective, this is an extreme case of the founder effect where the uninhabited area is settled by only one of the neutral fractions. Numerical results suggest that for compact initial conditions the spread is still dominated by the leading neutral fraction. The setback is that we do not know exactly how fast compact initial conditions converge to the traveling wave solution, but the proof of Theorem 1 suggests that solutions starting with initial conditions spread at most like $c^*t - 1/2 \ln(t)$. Hence, we are only able to show that for compact initial conditions that spread at c^*, all neutral fractions will be outrun by the moving half-frame, see Corollary 1.

When the growth function has a strong Allee effect, we are able to show that asymptotically each neutral fraction converges to a proportion of the traveling wave solution given by Eq. (36). The proportion of individuals is dependent on the initial condition of the neutral fractions, the traveling wave solution, and the asymptotic

spreading speed of the population. It is also clear from Eq. (36) that the neutral fractions at the wave front contribute a larger proportion of the total population density than those at the rear. This is analogous with the concept of a pushed front, where the genetic variation at the front of the wave comes from the spill over effect from the strong Allee effect. Generally, the Allee effect is thought to have a negative connotation on expanding populations because of the ability of the population to die out for low density levels. Our results show that the strong Allee effect preserves the neutral genetic variation in an expanding population. Thus, the strong Allee effect has a positive effect on the neutral genetic variation of an expanding population. We did not generalize this result for the general class of thin-tailed dispersal kernels as done in the case where the per capita growth was maximal at zero.

The results proven in this paper can be connected to those for partial differential equations. When the dispersal kernel is Gaussian with mean zero, we are able to compare the results of Theorems 1 and 2 to the previous results for reaction diffusion equations (Garnier et al. 2012; Roques et al. 2012). The conclusions from Theorem 1 are the same as for reaction diffusion equations where the growth function is of KPP type. When the growth function has a strong Allee effect, Theorem 2 predicts that each neutral fraction converges to a proportion of the traveling wave solution given by Eq. (36). This proportion is the same as the one calculated for the bistable reaction diffusion equation when k is $N(0, 2)$.

We were able to extend the results of Theorem 1 to thin-tailed dispersal kernels. This result is given by Theorem 3. Here, we see the same results as seen in the previous result for Gaussian kernels that the traveling wave solution is a pulled front and the spread is dominated by the leading neutral fraction. The proofs for Theorems 1 and 3 are very different because in the thin-tailed case we were not able to exploit the form of the moment generating function for Gaussian dispersal kernels. Thus, when inverting the bilateral Laplace transform, we could not use the convolution theorem to simplify the calculations and were left to compute the complex integral. The extension was not direct because we were forced to place an assumption allowing for our initial condition to be bounded by a function whose Fourier transform is in $L^1(\mathbb{R})$.

This theory provided by Theorems 1 and 3 requires that the per capita growth rate is maximal at zero. Thus, we are able to apply these results to growth functions with overcompensation such as the Ricker and logistic type growth. Growth functions with overcompensation can produce nonmonotone traveling wave solutions as seen in Fig. 2c. We conjecture that in this scenario the shape of the nonmonotone shape of the traveling wave does not change the inside dynamics results for pulled fronts. The ability to analyze how overcompensation affects the neutral genetic patterns of spread is a unique feature that differentiates our work from previous studies. These types of dynamics were not possible in the previous works due to the fact that the entire population spread was governed by a scalar continuous-time model. We see that the sole effect of overcompensation does not promote neutral genetic variation in an expanding population. Thus, the traveling wave solution for the population density is still classified as a pulled front because the spread is dominated by the leading neutral fraction.

The collective results provide a way of classifying traveling wave solutions of integrodifference equations in terms of pulled and pushed fronts. That is, if the spread

is dominated by the leading neutral fraction, then the traveling wave solution is a pulled front. If the leading edge of the spread includes components from many neutral fractions, then the traveling wave solution is a pushed front. In the case where we have a Gaussian dispersal kernel, we conjecture that a traveling wave solution can be determined simply by how fast the wave decays at the leading edge. This was stated in Conjecture 1 where the critical decay depends on the spreading speed and dispersal parameters.

Even though this work answers some of the interesting questions about neutral genetic patterns in populations undergoing a range expansion in discrete time, it is clear that there is still more work to be done. There is still room to extend the result of Theorem 2 to a general class of thin-tailed dispersal kernels. The inclusion of a fat-tailed dispersal kernel is known to produce accelerating traveling waves. Whether this occurs when the growth function has an Allee effect is still unknown. Another direction of future work is to consider what happens to solutions with fat-tailed dispersal. In this case, we have accelerating traveling waves meaning that the speed that the wave travels increases with time.

The convergence rate for compact initial conditions to traveling wave solution is not known for integrodifference equations. If such a result was known, then we would be able to alter the speed of the moving half-frame to extend this result as to never outrun the solution of System (13). This points toward the need for convergence theory about the speed of the solution approaching the traveling wave solution for integrodifference equations. For example, with partial differential equations, a well-known result by Bramson shows that in the frame of reference moving at $2t - \frac{3}{2}\ln(t) + x_\infty$, where x_∞ is dependent on the initial condition, the solution of the Fisher KPP equation converges as $t \to \infty$ to a translation of the traveling wave solution corresponding to the minimal asymptotic spreading speed $c^* = 2$ (Bramson 1983). This result gives us the exact speed needed for the moving frame to capture the solution for compact initial conditions in the reaction diffusion equation framework with KPP type growth.

Based on the assumption made on the decay of the initial condition in Theorem 1 and the decay traveling wave solution made in Theorem 2, we make the following conjecture for the classification of traveling wave solutions to Eq. (1).

Conjecture 1 (Decay properties of Gaussian traveling waves) *Consider a traveling wave solution $U(x - ct)$, to Eq. (1) with a Gaussian dispersal kernel. If we have that $\int_{-\infty}^{\infty} e^{\frac{c-\mu}{\sigma^2}y} U(y)\,dy < \infty$ (U decays faster than $e^{\frac{c-\mu}{\sigma^2}y}$) then $U(x - ct)$ is a pushed front. If we have that $U(x - ct)$ decays exactly at the exponential rate $e^{\frac{c-\mu}{\sigma^2}y}$, then $U(x - ct)$ is a pulled front solution corresponding to the minimum asymptotic spreading speed $c^* = \sqrt{2\sigma^2 \ln(g(0))} + \mu$. If $U(x - ct)$ decays slower than $e^{\frac{c-\mu}{\sigma^2}y}$, then $U(x - ct)$ is a pulled front with speed $c > c^*$.*

If Conjecture 1 is true, then it could give insight to the issue of pushed versus pulled fronts for growth functions with a weak Allee effect. Moreover, Conjecture 1 suggests the critical decay rate for differentiating traveling wave solutions as pulled or pushed fronts.

Outside of the realm of the inside dynamics analysis, this work also motivates future work for many general questions about traveling wave solutions for integrodifference

equations. The open questions that we encountered for integrodifference equations when completing this work were as follows:

1. What are the asymptotic decay properties for traveling wave solutions?
2. How fast do pulled front solutions with compact initial conditions approach the traveling wave solution?
3. What is the asymptotic spreading speed for growth functions with a strong Allee effect?

In summary, our work presents a framework for understanding the neutral genetic consequences of a population with nonoverlapping generations undergoing a range expansion. By connecting the ecological concepts with a mathematical model we encounter many interesting mathematical problems. The results shown in Sect. 3 provide an excellent start to understanding the question of interest; however, there are many questions that we were not able to answer due to limited mathematical theory. Therefore, with improved mathematical theory we can provide better insight to understanding the neutral genetic diversity of expanding populations.

Appendix

Proof of Lemma 1

Proof For simplicity in notation we focus on a single neutral fraction and drop the superscript i notation. By assumption, $x^2 v_0(x) e^{sx} \in L^1(\mathbb{R}) \cap L^\infty(\mathbb{R})$. Thus, we have

$$x^2 v_0(x) e^{sx} \le (1 + x^2) v_0(x) e^{sx} \le C \tag{93}$$

for all $x \in \mathbb{R}$ where C is a positive constant. Rearranging the previous inequality,

$$v_0(x) \le \frac{C e^{-sx}}{1 + x^2} \tag{94}$$

for all $x \in \mathbb{R}$. Thus, there exists a positive constant C such that the function $w_0(x)$ defined by

$$w_0(x) := \frac{C e^{-sx}}{1 + x^2} \tag{95}$$

satisfies $v_0(x) \leq w_0(x)$ for all $x \in \mathbb{R}$. It is easy to see that $w_0(x)e^{sx} \in L^1(\mathbb{R}) \cap L^\infty(\mathbb{R})$. Hence, the Fourier transform of $w_0(x)e^{sx} \in L^1(\mathbb{R})$. To calculate the Fourier Transform of $w_0(x)e^{sx}$, note that

$$\mathcal{F}\left[e^{-|x|}\right](\omega) = \int_{-\infty}^{\infty} e^{-|x|}e^{-i\omega x}\,dx \tag{96}$$

$$= \int_{-\infty}^{0} e^{(1-i\omega)x}\,dx + \int_{0}^{\infty} e^{-(1+i\omega)x}\,dx \tag{97}$$

$$= \lim_{b\to\infty}\left[\frac{e^{(1-i\omega)x}}{(1-i\omega)}\bigg|_{-b}^{0} - \frac{e^{-(1+i\omega)x}}{(1+i\omega)}\bigg|_{0}^{b}\right] \tag{98}$$

$$= \lim_{b\to\infty}\left[\frac{1}{(1-i\omega)} - \frac{e^{-(1-i\omega)b}}{(1-i\omega)} - \frac{e^{-(1+i\omega)b}}{(1+i\omega)} + \frac{1}{(1+i\omega)}\right] \tag{99}$$

$$= \left[\frac{1}{(1-i\omega)} + \frac{1}{(1+i\omega)}\right] \tag{100}$$

$$= \frac{2}{1+\omega^2}. \tag{101}$$

From the inverse Fourier transform,

$$\pi e^{-|x|} = \frac{\pi}{2\pi}\int_{-\infty}^{\infty}\frac{2}{1+\omega^2}e^{i\omega x}\,d\omega \tag{102}$$

$$= \int_{-\infty}^{\infty}\frac{1}{1+\omega^2}e^{i\omega x}\,d\omega. \tag{103}$$

Using the above result,

$$\mathcal{F}\left[\frac{C}{1+x^2}\right](\omega) = \mathcal{F}\left[\frac{C}{1+(-x)^2}\right](\omega) \tag{104}$$

$$= C\int_{-\infty}^{\infty}\frac{1}{1+(-x)^2}e^{-i\omega(-x)}\,dx \tag{105}$$

$$= C\int_{-\infty}^{\infty}\frac{1}{1+x^2}e^{i\omega x}\,dx \tag{106}$$

$$= C\pi e^{-|\omega|}. \tag{107}$$

The proof of the lemma is complete. $\qquad\square$

References

Bonnefon O, Garnier J, Hamel F, Roques L (2013) Inside dynamics of delayed traveling waves. Math Model Nat Phenom 8(3):42–59

Bonnefon O, Coville J, Garnier J, Roques L (2014) Inside dynamics of solutions of integro-differential equations. Discret Continu Dyn Syst Ser B 19(10):3057–3085

Bramson M (1983) Convergence of solutions of the Kolmogorov equation to travelling waves, vol 285. American Mathematical Society, Providence

Casella G, Berger RL (2002) Statistical inference, vol 2. Duxbury, Pacific Grove

Dlugosch KM, Parker I (2008) Founding events in species invasions: genetic variation, adaptive evolution, and the role of multiple introductions. Mol Ecol 17(1):431–449

Excoffier L (2004) Patterns of dna sequence diversity and genetic structure after a range expansion: lessons from the infinite-island model. Mol Ecol 13(4):853–864

Excoffier L, Ray N (2008) Surfing during population expansions promotes genetic revolutions and structuration. Trends Ecol Evol 23(7):347–351

Garnier J, Giletti T, Hamel F, Roques L (2012) Inside dynamics of pulled and pushed fronts. J Math Pure Appl 98(4):428–449

Hallatschek O, Nelson DR (2008) Gene surfing in expanding populations. Theor Popul Biol 73(1):158–170

Hallatschek O, Hersen P, Ramanathan S, Nelson DR (2007) Genetic drift at expanding frontiers promotes gene segregation. Proc Natl Acad Sci 104(50):19926–19930

Hewitt GM (1996) Some genetic consequences of ice ages, and their role in divergence and speciation. Biol J Linn Soc 58(3):247–276

Hewitt G (2000) The genetic legacy of the quaternary ice ages. Nature 405(6789):907–913

Holmes EE, Lewis MA, Banks J, Veit R (1994) Partial differential equations in ecology: spatial interactions and population dynamics. Ecology 75(1):17–29

Ibrahim KM, Nichols RA, Hewitt GM (1996) Spatial patterns of genetic variation generated by different forms of dispersal. Heredity 77:282–291

Kot M (1992) Discrete-time travelling waves: ecological examples. J Math Biol 30(4):413–436

Krasnosel'skii MA, Zabreiko PP (1984) Geometrical methods of nonlinear analysis. Springer, Berlin

Lewis MA, Petrovskii SV, Potts JR (2016) The mathematics behind biological invasions, vol 44. Springer, Berlin

Li B, Lewis MA, Weinberger HF (2009) Existence of traveling waves for integral recursions with non-monotone growth functions. J Math Biol 58(3):323–338

Lui R (1983) Existence and stability of travelling wave solutions of a nonlinear integral operator. J Math Biol 16(3):199–220

Lutscher F (2008) Density-dependent dispersal in integrodifference equations. J Math Biol 56(4):499–524

Mayr E (1942) Systematics and the origin of species, from the viewpoint of a zoologist. Harvard University Press, Harvard

Müller MJ, Neugeboren BI, Nelson DR, Murray AW (2014) Genetic drift opposes mutualism during spatial population expansion. Proc Natl Acad Sci 111(3):1037–1042

Ricker WE (1954) Stock and recruitment. J Fish Board Can 11(5):559–623

Roques L, Garnier J, Hamel F, Klein EK (2012) Allee effect promotes diversity in traveling waves of colonization. Proc Natl Acad Sci 109(23):8828–8833

Rothe F (1981) Convergence to pushed fronts. Rocky Mt J Math 11(4):617–634

Slatkin M, Excoffier L (2012) Serial founder effects during range expansion: a spatial analog of genetic drift. Genetics 191(1):171–181

Stokes A (1976) On two types of moving front in quasilinear diffusion. Math Biosci 31(3–4):307–315

Thomas CD, Bodsworth E, Wilson RJ, Simmons A, Davies ZG, Musche M, Conradt L (2001) Ecological and evolutionary processes at expanding range margins. Nature 411(6837):577–581

Thompson GG (1993) A proposal for a threshold stock size and maximum fishing mortality rate. Can Spec Publ Fish Aquat Sci 120:303–320

Vladimirov VS (1971) Equations of mathematical physics (Uravneniia matematicheskoi fiziki). Marcel Dekker, New York

Wang MH, Kot M, Neubert MG (2002) Integrodifference equations, Allee effects, and invasions. J Math Biol 44(2):150–168

Weinberger H (1982) Long-time behavior of a class of biological models. SIAM J Math Anal 13(3):353–396

Zemanian AH (1968) Generalized integral transformations, vol 140. Interscience, New York